

Accepted Manuscript

Electrochemical behaviour of dipyrone (metamizole) and others pyrazolones

Raphael P. Bacil, Rafael M. Buoro, Othon S. Campos, Matesa A. Ramos, Caroline G. Sanz, Silvia H.P. Serrano



PII: S0013-4686(18)30826-0

DOI: [10.1016/j.electacta.2018.04.082](https://doi.org/10.1016/j.electacta.2018.04.082)

Reference: EA 31649

To appear in: *Electrochimica Acta*

Received Date: 24 January 2018

Revised Date: 9 April 2018

Accepted Date: 11 April 2018

Please cite this article as: R.P. Bacil, R.M. Buoro, O.S. Campos, M.A. Ramos, C.G. Sanz, S.H.P. Serrano, Electrochemical behaviour of dipyrone (metamizole) and others pyrazolones, *Electrochimica Acta* (2018), doi: 10.1016/j.electacta.2018.04.082.

This is a PDF file of an unedited manuscript that has been accepted for publication. As a service to our customers we are providing this early version of the manuscript. The manuscript will undergo copyediting, typesetting, and review of the resulting proof before it is published in its final form. Please note that during the production process errors may be discovered which could affect the content, and all legal disclaimers that apply to the journal pertain.

Electrochemical behaviour of dipyron (metamizole) and others pyrazolones

Raphael P. Bacil^a, Rafael M. Buoro^b, Othon S. Campos^a, Matesa A. Ramos^a,
Caroline G. Sanz^a, Silvia H. P. Serrano^{a*}.

^a Department of Fundamental Chemistry, Institute of Chemistry – University of São Paulo, CEP: 05508-000, São Paulo (SP), Brazil

^b Department of Physics and Molecular Chemistry, São Carlos Institute of Chemistry – University of São Paulo, CEP: 13566-590 - São Carlos (SP), Brazil

Keywords: Dypirone; Metamizole; Antipyrines; Mechanism; Voltammetry;

*Email: shps@iq.usp.br

Abstract

The electrochemical oxidation of dipyrone (MTM) in aqueous medium was characterized using antipyrine (AA), 4-aminoantipyrine (4AA), 4-methylaminoantipyrine (MAA) and 4-dimethyl-aminoantipyrine (DMAA) as model molecules for the elucidation of all MTM voltammetric signals.

The MTM and the other pyrazolones show up to four oxidation electrochemical processes. The voltammograms obtained in AA solutions presented an irreversible electrochemical oxidation process involving one electron at E_{ap_3} , which is common to all pyrazolone derivatives, while the amino pyrazolones present electrochemical oxidation processes at E_{ap_0} or E_{ap_1} . The stabilization of the oxidation products depends on different effects: the proton release added to the thermodynamic stability, in the case of the imine formation at E_{ap_0} (4AA and MAA) and the hyperconjugation (σ -stabilization) in the case of iminium formation (DMAA and MTM) at E_{ap_1} . The process observed at E_{ap_0} corresponds to the pH-dependent oxidation of the primary and secondary enamines, while the process observed at E_{ap_1} occurs in the tertiary enamines, is pH independent. The oxidation peak potential follows the order: MAA < 4AA < DMAA < MTM and it was demonstrated that DMAA in an aqueous medium can simulate the MTM in an aprotic medium; therefore, the analytical MTM determination can be performed using the DMAA aqueous analytical curve. DMAA and MTM analytical curves, presented a linear range from 10 $\mu\text{mol L}^{-1}$ to 100 $\mu\text{mol L}^{-1}$ with a LOD of 1.94 and 2.97 μM for DMAA and MTM, respectively, LOQ of 6.48 and 9.91 μM ($n = 10$) and, sensitivity of 0.96 $\mu\text{A}/\mu\text{M}$ for DMAA and 0.92 $\mu\text{A}/\mu\text{M}$; with a recoveries of 95 to 105% for MTM.

1. Introduction

The antipyridines or pyrazolones are a group of the first synthesized pharmaceuticals to work as analgesics and antipyretics. The antipyrine (1,5-dimethyl-2-phenylpyrazol-3-one), **AA**, was the first one made by Knorr, thus, getting the group name. Some time after, other drugs were made, until they reached the aminoantipyrine (4-amino-1,5-dimethyl-2-phenylpyrazol-3-one), **4AA**; the dimethylaminoantipyrine, a.k.a. pyramidon, (4-(dimethylamino)-1,5-dimethyl-2-phenylpyrazol-3-one), **DMAA** and finally, [(1,5-dimethyl-3-oxo-2-phenylpyrazol-4-yl)-ethylamino] methanesulfonic acid], known as metamizole or dipyrone, **MTM**, an injectable formulation with antipyretic and analgesic effects [1].

MTM undergoes a hydrolysis reaction and generates the 4-methylamino antipyrine, **MAA** [2–4], which is enzymatically metabolized in the liver producing other metabolites, such as 4-amino-2,3-dimethyl-1-phenyl-3-pyrazol-5-one, **FAA** and 4-dimethylamino-1,5-dimethyl-2-phenylpyrazol-3-one, **AAA**[4, 5], **Schemes 1 and 2**.

INSERT SCHEME 1

INSERT SCHEME 2

The analgesic effect observed for MTM, as well as for other pyrazolones, is attributed to the inhibition of the cyclooxygenase enzyme (COX), in the liver, by the pharmacologically active metabolite, MAA [6, 7]; despite that, the inhibition mechanism of cyclooxygenase by the MTM is still unknown. Besides the COX hindering, the MTM and other pyrazolones can induce circumstantial allergic responses, such as Stevens–Johnson’s syndrome [8], rhinoconjunctivitis [9–11] and cause agranulocytosis[2, 8]. Still, MTM is in worldwide use [2, 3, 12–14].

Most studies dedicated to pyrazolones aim at their analytical detection. MTM gets more attention due to its high utilization, being determined and quantified by a variety of techniques, such as HPLC [15, 16], iodometry [17], FIA systems with amperometric detection [18–20], spectrophotometry, also associated with FIA systems by the addition of various reagents [21–23], capillary electrophoresis [24], NMR [16] and voltammetry [25–29]. AA is determined by HPLC [30–32], gas chromatography [33], NMR [34] and voltammetry [35–37]. Pyramidon also gets attention in some papers, such as HPLC with amperometric detection [30,38], voltammetry [36], NMR [39] and a CG method utilized to detect DMAA in apprehended samples of cocaine, in which it is used as adulterant [40].

On an electrochemical overview, several studies were carried out with different types of electrodes, our group utilized a glassy carbon electrode in previous studies [2], Marcolino et al. [25] utilized carbon paste electrodes as working electrode, as well as, Teixeira et al. [35], which modifies the carbon paste with *N,N'*-ethylenebis(salicylideneaminato)oxovanadium(IV), and Cumba et al. [41], who utilized a carbon paste modified with a composite titanium phosphate/nickel hexacyanoferrate. Metallic electrodes were also utilized, Basaez et al. [29] used platinum electrodes and Munoz et al. [42] disposable gold electrodes obtained from recordable CDs. The difference between carbon-based electrodes and metallic or metallic composites electrodes are the different potential windows and the electrochemical processes definitions. Therefore, carbon-based, such as glassy carbon electrodes, present a most adequate potential window to the electrochemical pyrazolones' oxidation mechanism study providing a constant surface for the electrochemical oxidation without surface passivation problems due to oxide formations in multiple scans, which can give an

indirect response to the analyte through interactions with the formed oxide that are independent of the molecule itself, a problem in both platinum and gold electrodes.

The aim of this work was to study the electrochemical oxidation of MTM in an aqueous medium, using AA, 4AA, MAA and DMA as model molecules for the elucidation of all MTM voltammetric signals and to understand why the oxidation peak potentials are different although the oxidation sites are the same in all molecules, except AA.

Using this strategy, it was possible not only to understand but also to describe, the electrochemical oxidation mechanism and reactivity of MTM and other biologically active pyrazolones, as well as the probable inhibition mechanism of the COX enzyme.

2. Experimental

2.1. Reagents and Solutions

All reagents were of analytical grade without any previous purification. The solutions were prepared using deionized water from a reverse osmosis device (Gehara Co., model OS10LX ultra-pure system, water resistivity $\geq 18 \text{ M}\Omega \text{ cm}$). Phosphate buffer solutions (PBS), 0.1 mol L^{-1} , were prepared by mixing appropriate amounts of H_3PO_4 and NaH_2PO_4 (Merck) in deionized water. Similar procedures were used to prepare the AA (Sigma Aldrich, code D-8890), 4AA (Sigma Aldrich, code A-4382), DMAA (Sigma Aldrich, code D8015) and MTM (Sigma Aldrich, code D-8890) solutions. The pH adjustments to the desired pH were performed by the addition of 4.0 mol L^{-1} NaOH solution. The supporting electrolyte used in the organic medium (DMF - Sigma Aldrich, code 227056) was 0.1 mol L^{-1} tetrabutylammonium tetrafluoroborate (TFBTBA - Merck code 8.18244.0025). All experiments were performed at room

temperature (25 ± 1 °C) and micro volumes were measured using EP-10 and EP-100 Unipette microliter pipettes (Uniscience, Brazil).

2.2. Obtainment and Characterization of MAA

MAA was obtained by hydrolysis of 10 mmol L^{-1} MTM solutions at 80 °C for 2 h under vigorous stirring. The MAA was extracted from the solution with chloroform and obtained in the solid form, after rotation evaporation of the solvent. It was resolubilized in CDCl_3 to perform the NMR essays.

2.3. Apparatus

All voltammograms were obtained using a PGSTAT 101 potentiostat/galvanostat, Metrohm AUTOLAB, connected to an IME663 interface stirrer device. The data treatment was performed with NOVA software version 1.10.4. and Origin 8.0. Glassy carbon electrode (GCE – $3 \text{ mm } \phi$), Ag/AgCl, KCl(sat) and a platinum wire were used as working, reference and auxiliary electrodes, respectively, in a 20 mL electrochemical cell. All pH measurements were performed using a pH meter model 654 and a combined glass electrode, model 6.0203.100 (OE), both from Metrohm.

The spectrophotometric measurements were performed with an Agilent 8453 spectrophotometer with the Chem Station software from Agilent Technologies. The high-performance liquid chromatograms were obtained using a Shimadzu HPLC system LC 10 with UV–vis detection and the data treatment performed with a software HPLC class LC 10. NMR spectra were obtained in a Bruker 500 MHz equipment with ACS labs software. All data were obtained at room temperature, 25 ± 3 °C.

2.3.1. UV–vis Spectra

The UV and visible spectrophotometric measurements were performed using deuterium and tungsten lamps, respectively, and a quartz cuvette with 1.0 cm optical path. The blank spectra were performed in PBS, pH 7.4.

2.3.2. High-Performance Liquid Chromatography (HPLC)

The chromatograms were obtained with the Shimadzu Diode Array at 241 nm fixed wavelength using a reversed phase technique and analytical column of C18 (5.0 μm , 15 cm and 4.7 mm), previously coupled to a precolumn with a 1.0 μL loop. The mobile phase was methanol/PBS in a 55%/45% (V/V) proportion at pH 2.5 with a flow rate of 1.0 mL min^{-1} .

2.3.3. Nuclear Magnetic Resonance (NMR)

The ^1H and ^{13}C NMR spectra (500 MHz frequency) were obtained using a Bruker equipment, <http://ca.iq.usp.br>. The samples were prepared in CDCl_3 , a sequence pulse zg30 was utilized in both spectra. To compare quantitatively the ^1H and ^{13}C NMR spectra, a computational simulation was obtained using the software ChemBioDraw 2010.

2.3.4. Electrochemical Measurements

2.3.4.1. Glassy Carbon Surface Pretreatment

The GCE was polished using 1.0/0.1 μm size particle diamond spray (Buehler, US) in a metallographic felt (Buehler, US) to avoid superficial adsorption effects.

2.3.4.2. Cyclic Voltammetry (CV)

The voltammograms were performed using the following experimental conditions: $E_{\text{initial}} = 0.0 \text{ V}$; $E_{\lambda} = 1.4 \text{ V}$, $E_{\text{final}} = 0.0 \text{ V}$, step potential = 2.0 mV and $\nu = 100.0 \text{ mV s}^{-1}$. The solutions were stirred before each measurement. Distinct conditions in any assay are specified in the figure caption.

2.3.4.3. Square Wave Voltammetry (SWV)

The SW voltammograms were obtained using the following experimental conditions: $E_{\text{initial}} = 0.0$ V; $E_{\text{final}} = 1.4$ V; step potential = 2.0 mV, pulse amplitude = 50.0 mV, frequency = 25.0 Hz, resulting in scan rate $\nu = 50.0$ mV s⁻¹. The solutions were stirred before each measurement.

2.3.4.4. Differential Pulse Voltammetry (DPV)

The experimental conditions for DPV experiments were: $E_{\text{initial}} = 0.0$ V, $E_{\text{final}} = 1.4$ V; pulse amplitude = 50 mV; pulse width = 100.0 ms; step potential = 2.5 mV and interval time = 0.5 s resulting in scan rate of 5 mV s⁻¹. The solutions were stirred before each measurement.

3. Results and Discussion

3.1. Electrochemical Characterization of MTM and the Other Pyrazolones

Cyclic voltammograms obtained in the antipyrine solutions show up to four oxidation processes ($E_{\text{ap}0}/E_{\text{ap}1}$, $E_{\text{ap}2}$, $E_{\text{ap}2'}$ and $E_{\text{ap}3}$), Figure 1. The voltammograms obtained in AA solutions presented only $E_{\text{ap}3}$ process because this molecule has no substituents on the pyrazolone ring; therefore, the most plausible oxidation possibility is in the nitrogen atom, adjacent to the aromatic ring, in a similar mechanism observed for acetaminophen [43], **Figure 1A**. The other molecules (4-AA, MAA, DMA and MTM) have an enamine moiety (group $-\text{C}=\text{C}-\text{N}-$) as a substituent of the pyrazolone ring, **Scheme 1**. The comparison between the voltammograms presented in **Figure 1A** with those on **Figures 1B–1E** permit the conclusion that the oxidation processes in these molecules involve the enamine moiety.

Insert Figure 1

Probably, the oxidation processes E_{ap_0} (4AA and MAA) and E_{ap_1} (DMAA and MTM) occur in the enamine itself; however, the oxidation products obtained in E_{ap_0} and E_{ap_1} differ in stability and the more stable the product, the less positive is the oxidation peak potential, **Table 1**.

Insert Table 1

Table 1 shows that the oxidation peak potential follows the order $MAA < 4AA < DMAA < MTM$. The first oxidation processes of 4AA and MAA (at E_{ap_0}) are irreversible and pH dependent, **Figures 1 and 2**, while for DMAA and MTM, the first oxidation process at E_{ap_1} is pH independent and shows a small cathodic component in the reverse scan, **Figure 1E**. According to the slope of the Pourbaix diagrams, 0.054 V/pH and 0.055 V/pH for 4AA and MAA, respectively, both oxidation processes occur involving the same number of electrons and protons and, the experimental pK_a value for both molecules is 7.4, **Figure 2**.

Insert Figure 2

To estimate the number of electrons involved in the oxidation processes, differential pulse voltammograms were obtained with GCE in aqueous and nonaqueous media and the data are presented in **Figures 3, 4 and Table 2**. The E_{ap_0} peak obtained for 4AA (**Figure 3B**) and MAA (**Figure 3C**) can be mathematically deconvoluted to distinguish the involved processes. Two distinct peaks were obtained: E_{ap_0} the first one, which corresponds to the oxidation of the enamine (**red line, Figure 3B**) to the corresponding imine, which can undergo a hydrolysis, resulting in a product that can also be oxidized [44] (**green line, Figure 3B and red line on Figure 3C**).

Insert Figure 3

To avoid water-dependent coupled chemical reactions, differential pulse voltammograms were also obtained in DMF containing 0.1 mol L^{-1} TFBTBA solution.

It would have been expected that, in the absence of water, the pH-dependent oxidation peak potentials, which occur in the same moiety of the molecule, to have similar oxidation potentials, as in fact occurred for E_{ap_0} and E_{ap_1} peaks, Figure 4.

Insert Figure 4

Insert Table 2

Table 2 shows the peak width at half height ($w_{1/2}$) values obtained in nonaqueous media for all oxidation processes and, according to these data, E_{ap_0} (4AA and MAA) corresponds to a process involving one electron, given that the $w_{1/2}$ values were 89 and 107 mV, respectively. In the same medium, the $w_{1/2}$ values for DMAA and MTM at E_{ap_1} were 91 and 89 mV, respectively, which are close to the theoretical value (90 mV) for a charge transfer reaction involving one electron, typical of processes in which the oxidized products are radical species.

It is important to note that the E_{ap_0} value in **Figure 3E** is much less positive than the E_{ap_0} value in **Figure 4E**; this great difference can be explained by the number of protic species in the reaction medium in which the measurements were taken. E_{ap_0} in **Figure 3E** corresponds to the MAA oxidation from MTM hydrolysis; the oxidation process is proton-dependent and facilitated in an aqueous medium. DMF always contains a small amount of water and the MTM hydrolysis process is expected to occur, although to a small extent, but due to the low water content, the pH-dependent oxidation process will be difficult and observed at more positive potentials.

To evaluate the reversibility of the E_{ap_0} and E_{ap_1} processes, square wave voltammograms were obtained and data are presented in **Figure 5**.

Insert Figure 5

As can be seen from Figure 5, only E_{ap_1} for DMAA has reversible character and this result can be associated with the difference in the substituents bonded to the

pyrazolones ring: a tertiary enamine in the case of DMAA and a secondary enamine in the case of MAA.

In the first case, the iminium cation radical formed at E_{ap1} can be stabilized by the hyperconjugation effect, improved by the hydrogens of two methyl groups (σ -stabilization) and therefore, can be reversibly reduced at E_{cp} . However, in the MAA, the electrochemical oxidation process is favored by the loss of one proton and enhanced by the thermodynamic stability of the product, which confers a less positive oxidation peak potential to the MAA. The E_{ap0} oxidation process for MAA (**Figure 3C**), shows that the broad peak can be mathematically deconvoluted into two peaks: E_{ap0} the first one, corresponds to the oxidation of the enamine to the respective imine radical ($\cdot\text{C}=\text{C}=\text{N}-\text{R}$), (**red line, Figure 3B**) [43], similarly to that observed during the formation of the Schiff's bases [45,46] and a small peak, corresponding to the oxidation of the hydrolysis imine radical product, formed in a coupled chemical reaction (**red line on Figure 3C**). This can be the main reason for the irreversibility of the process observed at E_{ap0} in the MAA molecule.

Note that a similar effect was observed for 4AA (**green line, Figure 3b**) and therefore, the product formed at E_{ap0} for 4AA suffers hydrolysis reaction and is subsequently oxidized, following a similar oxidation mechanism to MAA. The primary enamine in 4AA has no methyl substituent to stabilize the oxidation product, and then, the E_{ap0} has a more positive value than those observed for DMAA and MAA.

Finally, it is important to understand why the E_{ap1} , **Figure 3**, for the MTM has the most positive value of all molecules. This fact can be explained taking into account the presence of the sulfoxide group (an electronic acceptor) as a substituent in the enamine group, in relation to the other studied compounds, the stabilization of its oxidation product is difficult. The E_{ap0} , **Figure 4**, corresponds to the oxidation of MAA

coming from the MTM hydrolysis process, while the E_{ap2} oxidation process corresponds to the oxidation of the product formed at E_{ap1} , as previously demonstrated for MTM [2].

3.2. Mechanism Evaluation

The MTM first electrochemical oxidation occurs in the tertiary enamine without the presence of proton to produce an iminium cation radical, which can suffer a nucleophilic attack by water to produce another reactive intermediate. Thus, to evaluate the oxidation mechanism in the absence of a possible coupled reaction, cyclic voltammograms were obtained in DMF solutions containing TFBTBA as a supporting electrolyte, **Figure 6A** (full window) and **Figure 6B** (restricted window).

INSERT FIGURE 6

If the potential window is restricted to +0.7 V, where the electrochemical process at E_{ap2} does not occur, it was observed that i_{pa1}/i_{pc} increases with increasing scan rate, reaching a stable value of 0.75 at 100 mV s^{-1} . These results suggest that the product formed at E_{ap1} can, at high scan rate, be reduced at E_{pc} or be consumed, at low scan rates, by a coupled chemical reaction in an EC mechanism, Figure 7.

The process occurring at E_{pa1} is diffusion controlled throughout the scan range studied ($\log i_{pa1} = 0.483 \log \nu + 0.730$, $R^2 = 0.985$), while that occurring at E_{pa2} is diffusion controlled at higher scan rate [$\log i_{pa2} = 0.443 \log \nu + 0.974$, $R^2 = 0.982$ (for $90 \text{ mV s}^{-1} \leq \nu \leq 1000 \text{ mV s}^{-1}$)] and adsorption controlled at low scan rate [$\log I_{pa2} = 0.893 \log \nu + 0.091$, $R^2 = 0.947$ (for $10 \text{ mV s}^{-1} \leq \nu \leq 90 \text{ mV s}^{-1}$)], data not shown.

INSERT FIGURE 7

The diffusion regions, in both E_{pa1} and E_{pa2} , as well as the constant ratio i_{pa1}/i_{cp} , observed at high scan rates ($>100 \text{ mV s}^{-1}$), indicate an electrochemical–

electrochemical (EE) mechanism, which was previously studied [2]. The electrochemical mechanism at E_{ap1} changes as a function of the scan rate, which is characteristic of electrochemical processes followed by a coupled chemical reaction.

Figure 8 is a representation of the first MTM electrochemical process in nonaqueous medium. E_{ap1} increases linearly with increasing scan rate, ν , from 10 to 100 mV s^{-1} and the slope of the linear portion is 30 $\text{mV/decade } \nu$, which is expected for an EC process involving one electron, E_{ap1}/E_{cp} . It is important to note that there is a region in the plot where E_{ap1} is constant and near of 0.56 V. Below this value, for low scan rates, the peak potential values are lower, showing that the chemical coupled reaction is facilitating the electrochemical process.

INSERT FIGURE 8

The chemical step after the electrochemical process is most likely a dimerization because a nucleophilic attack in an organic medium is highly unlikely to occur. In addition, the slope obtained in the E_{ap1} vs $\log \nu$ plot is very close to the documented theoretical value, 29.9 $\text{mV}/\log \nu$ [47] as expected for a process involving a dimerization step. Thus, it is suggested that the coupled chemical reaction is that represented by equation 1, where the oxidation product of the MTM formed in E_{ap1} undergoes a dimerization process and, apparently, this species is inactive.



The possible reaction pathways after the electrochemical oxidation of MTM are illustrated in **Scheme 3**.

INSERT SCHEME 3

Table 3 compiles the voltammetric data for E_{ap0} , E_{ap1} , E_{ap2} and E_{ap3} in AA, 4AA, MAA, DMAA and MTM.

INSERT TABLE 3

Based on the data presented in Table 3, an oxidation mechanism, Scheme 4, was proposed for the electrochemical oxidations of all pyrazolones studied.

INSERT SCHEME 4

3.3. Analytical Application

As observed in the S1 and S2 Figures, MTM's hydrolysis occurs with fast kinetics; thus, it is difficult to use MTM as a standard to obtain an analytical curve. However, if the proposed mechanism is correct, it should be possible to use DMAA as a model molecule to substitute MTM, because both have the same E_{ap1} process.

To validate this hypothesis, an analytical curve was constructed utilizing DMAA in an aqueous medium and compared with another MTM curve in an organic medium. DMAA and MTM analytical curves, present a linear range from 10 $\mu\text{mol L}^{-1}$ to 100 $\mu\text{mol L}^{-1}$ with a limit of detection (LOD) of 1.94 and 2.97 μM for DMAA and MTM, respectively, limit of quantitation (LOQ) of 6.48 and 9.91 μM ($n = 10$) [48] and a sensitivity of 0.96 $\mu\text{A}/\mu\text{M}$ for DMAA and 0.92 $\mu\text{A}/\mu\text{M}$ for MTM, Table 4 and **Figure 9**. Using this approach, MTM was quantified in commercial formulations with a recovery of 95 to 105%, **Table 4**.

INSERT FIGURE 9

INSERT TABLE 4

The obtained recoveries are satisfactory, implying that the proposed mechanism is correct.

4. Conclusions

The pyrazolones, depending on their structure, may exhibit up to four electrochemical processes, E_{ap_0} or E_{ap_1} , E_{ap_2} , $E_{ap_2'}$ and E_{ap_3} . The E_{ap_3} process occurs in the pyrazolone ring. It involves an irreversible electron charge transfer and is common to all compounds of this class. The molecules with the enamine moiety present three electrochemical processes, in addition to E_{ap_3} .

The processes E_{ap_0} or E_{ap_1} , both involving one electron, occur in the same electroactive moiety, the enaminoic nitrogen, substituent of the pyrazolone ring, and these processes depend on two different effects: the hyperconjugation (σ -stabilization) in the case of iminium cation radical formation (DMAA and MTM) at E_{ap_1} , which electrochemical processes are pH independent and the proton release, added to the thermodynamic stability, in the case of the imine radical formation at E_{ap_0} (4AA and MAA).

The E_{ap_2} process, which occurs after the E_{ap_0} or E_{ap_1} processes, is irreversible, involves one electron and is not pH dependent. In MTM, the electrochemical oxidation at E_{ap_2} competes with a chemical dimerization reaction, just after E_{ap_1} . The electrochemical process is favored at high scan rates ($>90 \text{ mV s}^{-1}$), when the chemical step is not favored, **Scheme 3**. The complete electrochemical oxidation mechanism for several pyrazolones, which data were compiled in Table 3, is illustrated in **Scheme 4**.

Pharmaceutical samples of MTM were prepared in an organic medium and the drug was quantified using an aqueous DMAA analytical curve. Satisfying recoveries were obtained, which corroborates the proposed oxidation mechanism for these molecules.

The voltammetric study of the pyrazolone group allowed understanding the reactivity of the molecules and shows that at physiological pH, MAA (secondary enamine) is easily oxidized and can act as a good reducing agent, which is the probable reason for which the COX enzyme, with iron(III) in its peroxidase active site, is inhibited by the dipyrone.

5. Acknowledgements

The authors would like to thank São Paulo Foundation Research (FAPESP), CNPq (Process 140833/2016-1), CAPES for the financial support and to Kevin Dias, PhD student, for the valuable discussions. This work is dedicated to Professor Dr. P.V. Antonio William Oliveira Lima (*in memoriam*).

6. References

- [1] K. Brune, The early history of non-opioid analgesics, *Acute Pain*. 1 (1997) 33–40.
- [2] R.P. Bacil, R.M. Buoro, R.P. da Silva, D.B. Medinas, A.W.O. Lima, S.H.P. Serrano, Mechanism of Electro-Oxidation of Metamizole using Cyclic Voltammetry at a Glassy Carbon Electrode, *E C S Trans. Electrochem. Soc.* 43 (2012) 251–258.
- [3] L. Loginova, O. Konovalova, Test films for test-determinations on the base of reagents, immobilized in gelatinous gel, *Talanta*. 77 (2008) 915–923. doi:10.1016/j.talanta.2008.07.051.
- [4] H. Ergün, D. a C. Frattarelli, J. V. Aranda, Characterization of the role of physicochemical factors on the hydrolysis of dipyrone, *J. Pharm. Biomed. Anal.*

- 35 (2004) 479–487. doi:10.1016/j.jpba.2004.02.004.
- [5] M. Levy, E. Zylber-Katz, B. Rosenkranz, Clinical pharmacokinetics of dipyrone and its metabolites., *Clin. Pharmacokinet.* 28 (1995) 216–34. doi:10.2165/00003088-199528030-00004.
- [6] S.C. Pierre, R. Schmidt, C. Brenneis, M. Michaelis, G. Geisslinger, K. Scholich, Inhibition of cyclooxygenases by dipyrone., *Br. J. Pharmacol.* 151 (2007) 494–503. doi:10.1038/sj.bjp.0707239.
- [7] S. Bingham, P.J. Beswick, D.E. Blum, N.M. Gray, I.P. Chessell, The role of the cyclooxygenase pathway in nociception and pain, *Semin. Cell Dev. Biol.* 17 (2006) 544–554. doi:10.1016/j.semcd.2006.09.001.
- [8] M. Levy, Hypersensitivity to pyrazolones, *Thorax.* 55 (2000) 72S–74. doi:10.1136/thorax.55.suppl_2.S72.
- [9] J.C. Wessel, M. Matyja, M. Neugebauer, H. Kiefer, T. Daldrup, F.A. Tarbah, H. Weber, Characterization of oxalic acid derivatives as new metabolites of metamizol (dipyrone) in incubated hen's egg and human., *Eur. J. Pharm. Sci.* 28 (2006) 15–25. doi:10.1016/j.ejps.2005.11.010.
- [10] L.A. Pérez-Estrada, S. Malato, A. Agüera, A.R. Fernández-Alba, Degradation of dipyrone and its main intermediates by solar AOPs. Identification of intermediate products and toxicity assessment, *Catal. Today.* 129 (2007) 207–214. doi:10.1016/j.cattod.2007.08.008.
- [11] S. Bellegrandi, R. Rosso, G. Mattiacci, A. Zaffiro, F. Di Sora, F. Menzella, F. Aiuti, R. Paganelli, Combined immediate- and delayed-type hypersensitivity to metamizole., *Allergy.* 54 (1999) 88–90. <http://www.ncbi.nlm.nih.gov/pubmed/10195371> (accessed October 20, 2014).
- [12] E. Di Leo, E. Nettis, G.F. Calogiuri, A. Ferrannini, A. Vacca, Immediate

- rhinoconjunctivitis induced by metamizole: an allergic reaction?, *Allergy*. 65 (2010) 1070–1071. doi:10.1111/j.1398-9995.2009.02299.x.
- [13] I.M. Benseñor, To use or not to use dipyrone ? Or maybe , Central Station versus ER ? That is the question ..., *São Paulo Med. J.* 119 (2001) 190–191.
- [14] D.F. Feldmann, S. Zuehlke, T. Heberer, Occurrence, fate and assessment of polar metamizole (dipyrone) residues in hospital and municipal wastewater, *Chemosphere*. 71 (2008) 1754–1764. doi:10.1016/j.chemosphere.2007.11.032.
- [15] K. Müssig, A. Pfäfflin, H.-U. Häring, E.D. Schleicher, Dipyrone (metamizole) metabolites interfere with HPLC analysis of plasma catecholamines but not with the determination of urinary catecholamines., *Clin. Chem.* 52 (2006) 1829–31. doi:10.1373/clinchem.2006.071662.
- [16] H.Z. Senyuva, I. Aksahin, S. Ozcan, B.V. Kabasakal, Rapid, simple and accurate liquid chromatography-diode array detection validated method for the determination of dipyrone in solid and liquid dosage forms, *Anal. Chim. Acta*. 547 (2005) 73–77. doi:10.1016/j.aca.2004.12.053.
- [17] T.R.L.C. Paixão, R.C. Matos, M. Bertotti, Diffusion layer titration of dipyrone in pharmaceuticals at a dual-band electrochemical cell, *Talanta*. 61 (2003) 725–732. doi:10.1016/S0039-9140(03)00334-5.
- [18] A.C. Boni, A. Wong, R.A.F. Dutra, M.D.P.T. Sotomayor, Cobalt phthalocyanine as a biomimetic catalyst in the amperometric quantification of dipyrone using FIA, *Talanta*. 85 (2011) 2067–2073. doi:10.1016/j.talanta.2011.07.038.
- [19] L.H. Marcolino-Júnior, M.F. Bergamini, M.F.S. Teixeira, É.T.G. Cavalheiro, O. Fatibello-Filho, Flow injection amperometric determination of dipyrone in pharmaceutical formulations using a carbon paste electrode, *Farm.* 58 (2003) 999–1004. doi:10.1016/S0014-827X(03)00182-4.

- [20] T. Pérez-Ruiz, C. Martínez Lozano, V. Tomás, Flow-injection determination of Novalgin using amperometric detection at a glassy carbon electrode., *J. Pharm. Biomed. Anal.* 12 (1994) 1109–13. <http://www.ncbi.nlm.nih.gov/pubmed/7803560> (accessed October 20, 2014).
- [21] L.H. Marcolino, R.A. Sousa, O. Fatibello-Filho, F.C. Moraes, M.F.S. Teixeira, Flow-injection spectrophotometric determination of dipyrone in pharmaceutical formulations using ammonium molybdate as chromogenic reagent, *Anal. Lett.* 38 (2005) 2315–2326. doi:10.1080/15265160500316351.
- [22] M. Tubino, A.C. Biondo, M.M.D.C. Vila, L. Pezza, H.R. Pezza, Spot-test identification and rapid quantitative sequential analysis of dipyrone, *Eclat. Quim.* 35 (2010) 41–46.
- [23] W.T. Suarez, O.D. Pessoa-Neto, F.C. Vicentini, B.C. Janegitz, R.C. Faria, O. Fatibello-Filho, Flow Injection Spectrophotometric Determination of Dipyrone in Pharmaceutical Formulations Using Fe(III) as Reagent, *Anal. Lett.* 44 (2011) 340–348. doi:10.1080/00032719.2010.500777.
- [24] L. Basáez, I.M. Peric, P. a Jara, C. a Soto, D.R. Contreras, C. Aguirre, P. Vanýsek, Electrochemical and Electrophoretic Study of Sodium Metamizole, *J. Chil. Chem. Soc.* 53 (2008) 3–6.
- [25] I. Baranowska, P. Markowski, A. Gerle, J. Baranowski, Determination of selected drugs in human urine by differential pulse voltammetry technique, *Bioelectrochemistry.* 73 (2008) 5–10. doi:10.1016/j.bioelechem.2008.04.022.
- [26] B. Muralidharan, G. Gopu, C. Vedhi, P. Manisankar, Determination of analgesics in pharmaceutical formulations and urine samples using nano polypyrrole modified glassy carbon electrode, *J. Appl. Electrochem.* 39 (2009) 1177–1184. doi:10.1007/s10800-009-9782-9.

- [27] L.J. Li, L.J. Cheng, Z. Cai, S.M. Lan, X.F. Guo, Y.Q. Li, Determination of Metamizole Sodium by Cyclic Voltammetry Under Microwave Activation, *Chem. Res. Chinese Univ.* 26 (2010) 537–540.
- [28] B. Muralidharan, G. Gopu, C. Vedhi, P. Manisankar, Voltammetric determination of analgesics using a montmorillonite modified electrode, *Appl. Clay Sci.* 42 (2008) 206–213. doi:10.1016/j.clay.2007.11.005.
- [29] M.F.S. Teixeira, L.H. Marcolino-júnior, O. Fatibello-filho, E.R. Dockal, Voltammetric Determination of Dipyrone Using a N,N'-ethylenebis(salicylideneaminato)oxovanadium(IV) Modified Carbon-paste Electrode, 15 (2004) 803–808.
- [30] A. Burcinova, M. Tichi, V. Pacakova, K. Stulik, Application of amperometric detection to the high-performance liquid chromatographic determination of antipyrine and 4-aminoantipyrine in urine, *J. Chromatogr. B.* V. 455 (1988) 420–424.
- [31] S. Zuehlke, U. Duennbier, T. Heberer, Determination of Polar Drug Residues in Sewage and Surface Water Applying Liquid Chromatography - Tandem Mass Spectrometry, 76 (2004) 6548–6554.
- [32] E. Wang, J. Zhou, Simultaneous Determination of Aminopyrine and Antipyrine by Liquid Chromatography / Electrochemistry with a Parallel Dual Electrode, *Microchem. J.* 42 (1990) 259–266.
- [33] S. Lindgren, P. Collste, B. Norlander, F. Sjöqvist, Gas chromatographic assessment of the reproducibility of phenazone plasma half-life in young healthy volunteers., *Eur. J. Clin. Pharmacol.* 7 (1974) 381–385. doi:10.1007/BF00558211.
- [34] I. Wilson, J. Nicholson, M. Hofmann, Investigation of the human metabolism of

- antipyrine using coupled liquid chromatography and nuclear magnetic resonance spectroscopy of urine, *J. Chromatogr.* 617 (1993) 324–328. <http://www.sciencedirect.com/science/article/pii/037843479380507Z> (accessed October 21, 2014).
- [35] N. V Bashkatova, E.I. Korotkova, Y. a Karbainov, a Y. Yagovkin, a a Bakibaev, Electrochemical, quantum-chemical and antioxidant properties of antipyrine and its derivatives., *J. Pharm. Biomed. Anal.* 37 (2005) 1143–7. doi:10.1016/j.jpba.2004.11.046.
- [36] H. Yin, Y. Zhou, T. Liu, T. Tang, S. Ai, L. Zhu, Determination aminopyrine in pharmaceutical formulations based on APTS-Fe₃O₄ nanoparticles modified glassy carbon electrode, *J. Solid State Electrochem.* 16 (2011) 731–738. doi:10.1007/s10008-011-1418-4.
- [37] H. Sayo, M. Masui, Anodic oxidation of amines. Part III. Cyclic voltammetry and controlled potential electrolysis of 4-dimethylaminoantipyrine (4-dimethylamino-2,3-dimethyl-1-phenyl- Δ^3 -pyrazolin-5-one) in acetonitrile, *J. Chem. Soc., Perkin Trans. 2.* (1973) 1640–1645. doi:10.1039/P29730001640.
- [38] S. Zuehlke, U. Duennbier, T. Heberer, Determination of polar drug residues in sewage and surface water applying liquid chromatography-tandem mass spectrometry, *Anal. Chem.* 76 (2004) 6548–6554. doi:10.1021/ac049324m.
- [39] M.S. Caubet, A. Laplante, J. Caillé, J.L. Brazier, [13 C]Aminopyrine and [13 C]Caffeine Breath Test: Influence of Gender, Cigarette Smoking and Oral Contraceptives Intake, *Isotopes Environ. Health Stud.* 38 (2002) 71–77. doi:10.1080/10256010208033314.
- [40] S.F. Lapachinske, G.G. Okai, A. dos Santos, A.V. de Bairros, M. Yonamine, Analysis of cocaine and its adulterants in drugs for international trafficking

- seized by the Brazilian Federal Police, *Forensic Sci. Int.* 247 (2015) 48–53.
doi:10.1016/j.forsciint.2014.11.028.
- [41] L.R. Cumba, U.D.O. Bicalho, D.R. Silvestrini, D.R. Do Carmo, Preparation and Voltammetric Study of a Composite Titanium Phosphate/Nickel Hexacyanoferrate and Its Application in Dipyrone Determination, *Int. J. Chem.* 4 (2012). doi:10.5539/ijc.v4n2p66.
- [42] R.A.A. Muñoz, R.C. Matos, L. Angnes, Amperometric determination of dipyrone in pharmaceutical formulations with a flow cell containing gold electrodes from recordable compact discs, *J. Pharm. Sci.* 90 (2001) 1972–1977.
doi:10.1002/jps.1148.
- [43] D.J. Miner, J.R. Rice, R.M. Riggin, P.T. Kissinger, Voltammetry of acetaminophen and its metabolites, *Anal. Chem.* 53 (1981) 2258–2263.
doi:10.1021/ac00237a029.
- [44] J.M. Savéant, *Elements of Molecular and Biomolecular Electrochemistry: An Electrochemical Approach to Electron Transfer Chemistry*, John Wiley & Sons, Inc., Hoboken, NJ, USA, 2006. doi:10.1002/0471758078.
- [45] J. Joseph, G.A.B. Rani, Metal-Based Molecular Design Tuning Biochemical Behavior: Synthesis, Characterization, and Biochemical Studies of Mixed Ligand Complexes Derived From 4-Aminoantipyrine Derivatives, *Spectrosc. Lett.* 47 (2014) 86–100. doi:10.1080/00387010.2013.776087.
- [46] N. Raman, A. Kulandaisamy, C. Thangaraja, P. Manisankar, S. Viswanathan, C. Vedhi, Synthesis, structural characterisation and electrochemical and antibacterial studies of Schiff base copper complexes, *Transit. Met. Chem.* 29 (2004) 129–135. doi:10.1023/B:TMCH.0000019409.50574.0a.
- [47] D. Pletcher, *Instrumental Methods in Electrochemistry*, 1st ed., Woodhead

Publishing Limited, Southampton, 2001.

<http://books.google.com/books?hl=en&lr=&id=Q6CjAgAAQBAJ&oi=fnd&pg=PP1&dq=Instrumental+Methods+in+Electrochemistry&ots=SjBuoNFS7W&sig=WTGL4H8jY8OCaPLMoulGimWeADY>.

- [48] J.N. Miller, J.C. Miller, *Statistics and Chemometrics for Analytical Chemistry*, 6th ed., Pearson, Gosport, 2010. doi:10.1198/tech.2004.s248.

Figure 1. Cyclic voltammograms obtained with GCE in 0.1 M PBS, pH = 7.4, containing 1 mM of each of the compounds: AA (**A**); 4AA (**B**); MAA (**C**); DMAA (**D**); MTM (**E**). Experimental conditions: as described in the experimental section.

Figure 2. Pourbaix diagrams: E_{ap0} from MAA (red line) and 4AA (black line).

Figure 3. Differential pulse voltammograms obtained with GCE in 0.1 mol L⁻¹ PBS, pH 7.4, containing 1.0 mmol L⁻¹ of AA (**A**); 4AA (**B**); MAA (**C**); DMAA (**D**) and MTM (**E**). The peak width at half height values ($w_{1/2}$) were obtained after the voltammogram deconvolution processes (colored lines). Experimental conditions: as described in the experimental section.

Figure 4. Differential pulse voltammograms obtained with GCE in DMF containing 0.1 M of TFBTBA and 1.0 mmol L⁻¹ of A) AA; B) 4AA; C) MAA; D) DMAA; E) MTM. Deconvolution processes were performed, when necessary, to obtain the values of $w_{1/2}$. Experimental data are shown as black lines while deconvolutions are displayed as colored lines. Experimental conditions: as described in the experimental section.

Figure 5. Square wave voltammograms (SWV) obtained with GCE in 0.1 M PBS, pH = 7.4, containing 1.0 mM of each of the compounds: AA (**A**); 4AA (**B**); MAA (**C**); DMAA (**D**); MTM (**E**). (1) Total current; (2) forward current; (3) backward current. Experimental conditions: as described in the experimental section.

Figure 6. Cyclic voltammograms obtained with GCE in DMF containing 0.1 mol L⁻¹ of TFBTBA and 1.0 mmol L⁻¹ of MTM: 10 mV s⁻¹ (1); 50 mV s⁻¹ (2); 100 mV s⁻¹ (3); 500 mV s⁻¹ (4) and 1000 mV s⁻¹ (5); $E_0 = 0.0$ V; $E_\lambda = 1.4$ V; $E_f = 0.0$ V (**A**) and 10 mV s⁻¹ (1); 50 mV s⁻¹ (2); 100 mV s⁻¹ (3); 500 mV s⁻¹ (4) and 1000 mV s⁻¹ (5); $E_0 = 0.0$ V; $E_\lambda = 0.7$ V; $E_f = 0.0$ V (**B**)

Figure 7. i_{ap1} / i_{cp} ratio as a function of scan rate (v). Applied potential window restricted to the interval in which only the first electrochemical process occurs.

Figure 8. E_{ap_1} vs $\log \nu$ plot obtained in DMF containing 0.1 mol L^{-1} TFBTBA and 1.0 mmol L^{-1} MTM. ($E_{p_1} = 0.030 \log \nu + 0.495$, $R^2 = 0.975$)

Figure 9. DMAA and MTM analytical curves obtained in PBS pH 7.4 (**black line**) and DMF containing 0.1 mol L^{-1} of TFBTBA (**red line**), respectively. DMAA solutions in PB, pH = 7.4 (Black). Data obtained from square wave voltammograms in 10 to 100 $\mu\text{mol L}^{-1}$ range (average of five measurements).

$i_{p(\text{DMAA})}/\mu\text{A} = 0.96[\text{DMAA}]\mu\text{M} - 0.45$ ($R^2 = 0.998$) and $i_{p(\text{MTM})}/\mu\text{A} = 0.92[\text{MTM}]\mu\text{M} - 0.59$ ($R^2 = 0.998$).

Scheme 1. The MTM hydrolysis and its generated products.

Scheme 2. Structure of the pyrazolones studied in this work. The abbreviations, as well as, the letter on the molecule were maintained throughout the work.

Scheme 3. Schematic representation of the possible reaction pathways after the E_{ap_1} process.

Scheme 4. Electrochemical oxidation mechanism proposed for dipyrone and antipyrine molecules.

Table 1. Compilation of the results obtained from the cyclic voltammograms presented in **Figure 1**.

Table 2. Peak width half height ($w_{1/2}$) values obtained from the differential pulse voltammograms presented in Figure 4.

Table 3. Compilation of reversibility, number of electrons and pH-dependency of the electrochemical oxidations processes for the pyrazolone derivatives.

Table 4. Analytical parameters obtained for MTM quantification in commercial pharmaceutical samples using DMAA and MTM analytical curves.

Table 1: Oxidation peak potentials obtained from the cyclic voltammograms presented in Figure 1.

| Process/ Molecule | Eap ₀ / V | Eap ₁ / V | Eap ₂ / V | Eap ₃ / V |
|-------------------|----------------------|----------------------|----------------------|----------------------|
| AA | - | - | - | 1.25 |
| 4AA | 0.552 | - | - | 1.22 |
| MAA | 0.245 | - | - | 1.24 |
| DMAA | - | 0.444 | 0.67 | 1.25 |
| MTM | - | 0.578 | 0.903 | 1.27 |

Table 2: Peak width at half height ($w_{1/2}$) obtained from the differential pulse voltammograms presented in Figure 4.

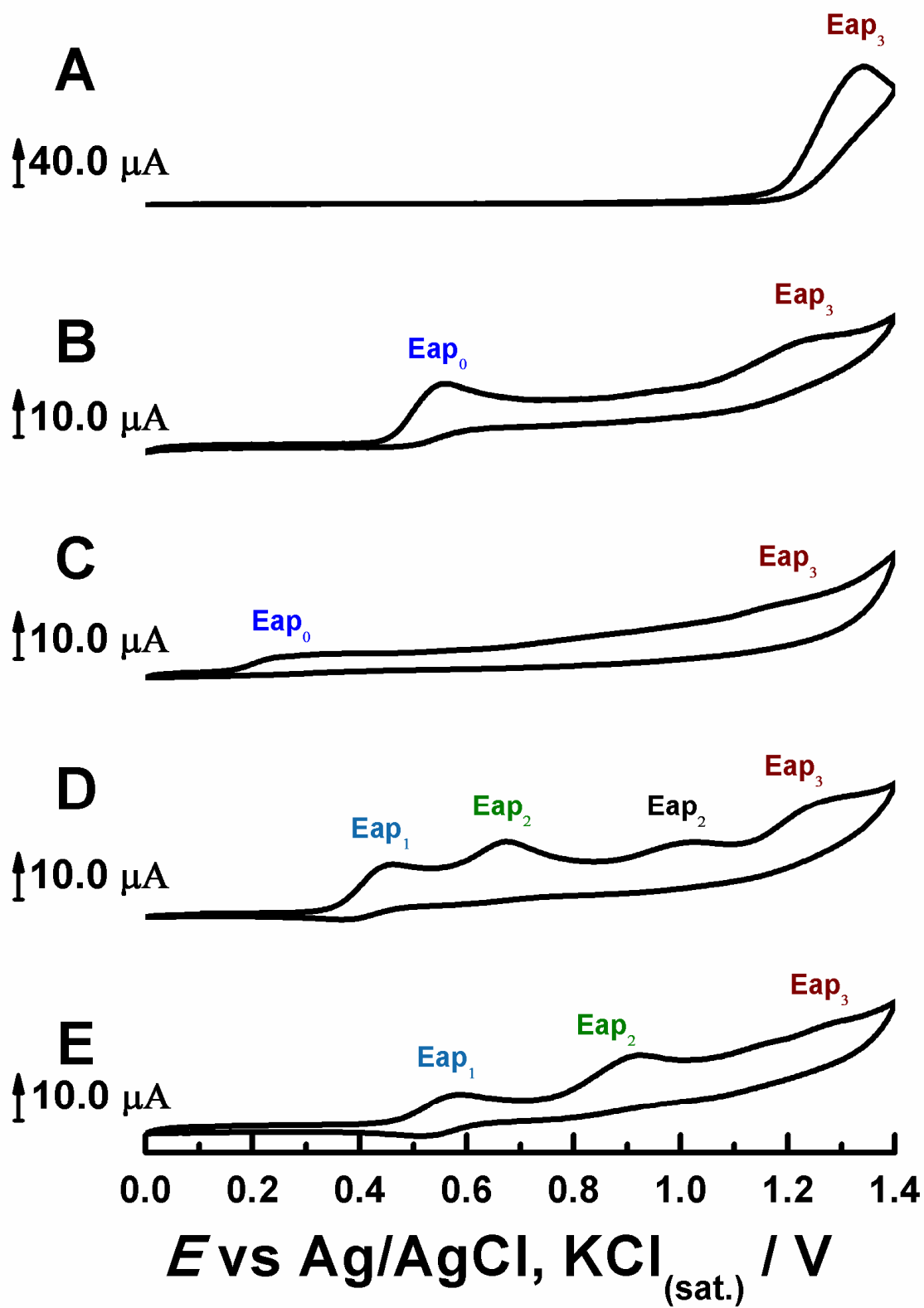
| $w_{1/2}$ | E_{ap0}/mV | E_{ap1}/mV | E_{ap2}/mV | E_{ap3}/mV |
|-----------|---------------------|---------------------|---------------------|---------------------|
| AA | - | - | - | 96 ± 6 |
| 4AA | 89 ± 3 | - | 99 ± 3 | 91 ± 5 |
| MAA | 107 ± 7 | - | 99 ± 6 | 110 ± 7 |
| DMAA | - | 91 ± 3 | 99 ± 4 | 102 ± 5 |
| MTM | - | 89 ± 4 | 99 ± 3 | 107 ± 6 |

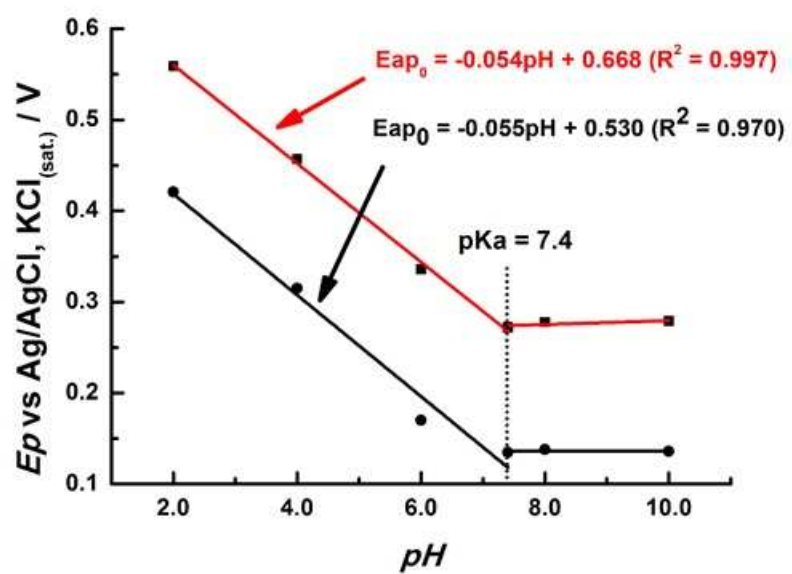
Table 3: Reversibility, number of the electrons and pH dependency of the electrochemical oxidation processes for the pyrazolone derivatives.

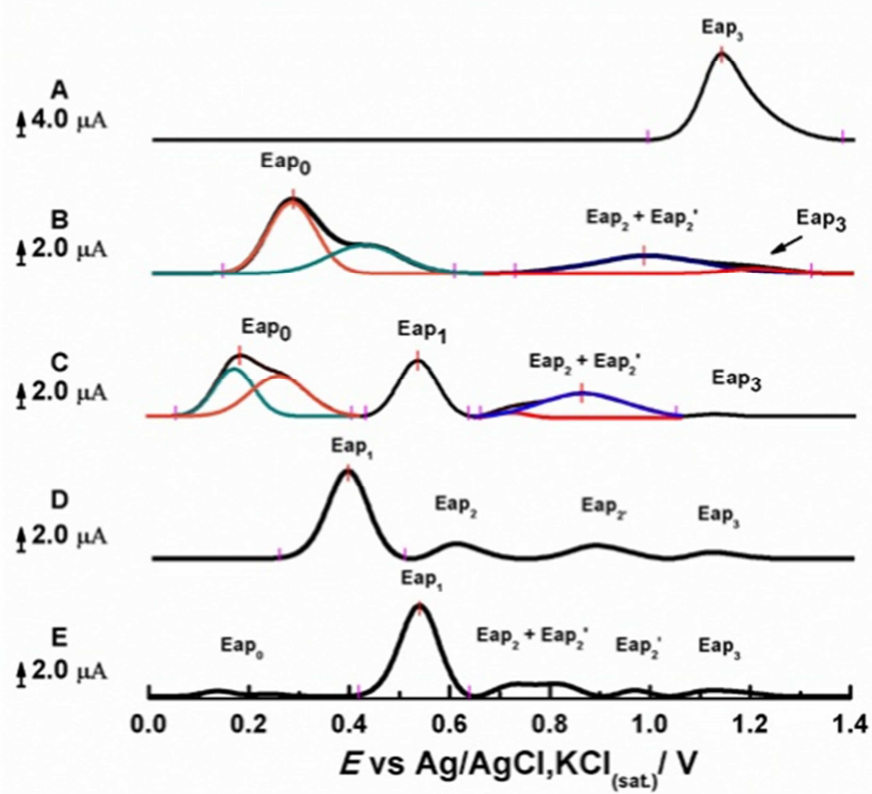
| Process | Molecule | Reversibility | n° of electrons | pH dependency |
|------------------|----------------------|---------------|-----------------|---------------|
| Eap ₀ | 4AA, MAA | No | 1 | Yes |
| Eap ₁ | DMAA, MTM | Yes | 1 | No |
| Eap ₂ | AA, 4AA, MAA, MTM | No | 1 | No |
| Eap ₃ | AA, 4AA, MAA, MTM | No | 1 | No |

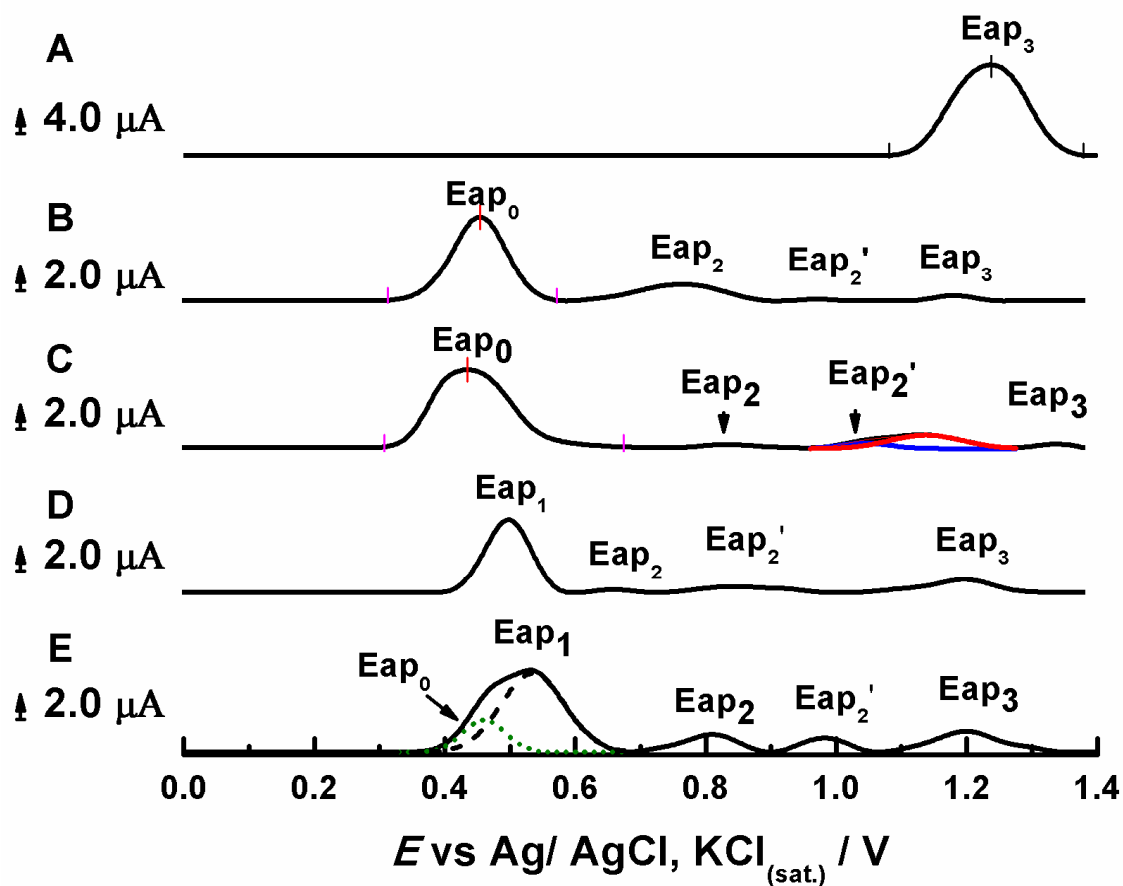
Table 4: Analytical parameters obtained for MTM Quantification in pharmaceutical samples using DMAA and MTM analytical curves

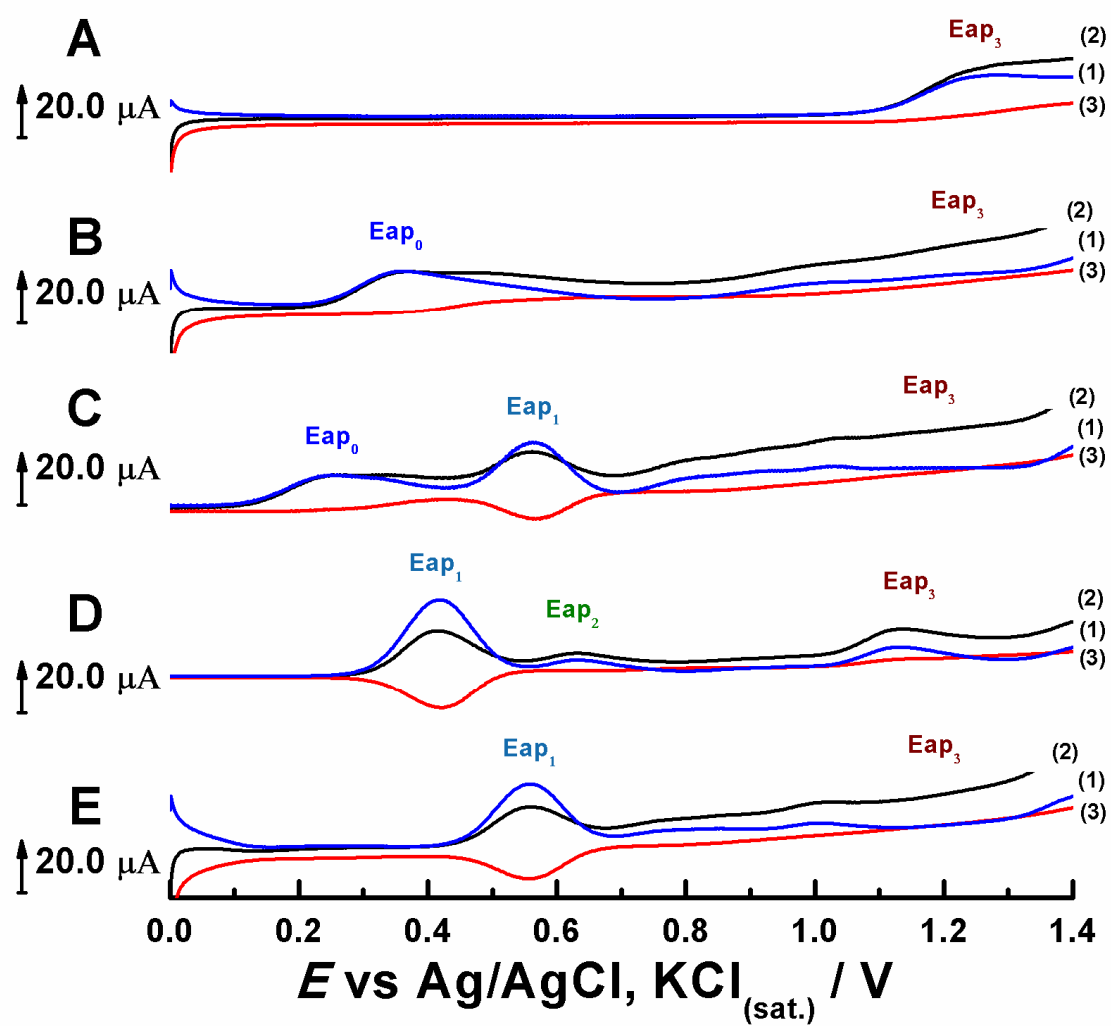
| Analytical Curve | Limit of detection ($\mu\text{mol L}^{-1}$) | Limit of quantification ($\mu\text{mol L}^{-1}$) |
|--------------------------|--|---|
| DMAA(PBS) | 1.94 | 6.48 |
| MTM (DMF) | 2.97 | 9.91 |
| Sample | Recovery - DMAA (%) | Recovery - MTM (%) |
| Novalgina TM | 95.0 | 86.2 |
| Dipyron (Medley) | 96.5 | 87.6 |
| Dorflex TM | 98.0 | 89.0 |
| Neosaldina TM | 105.0 | 95.2 |

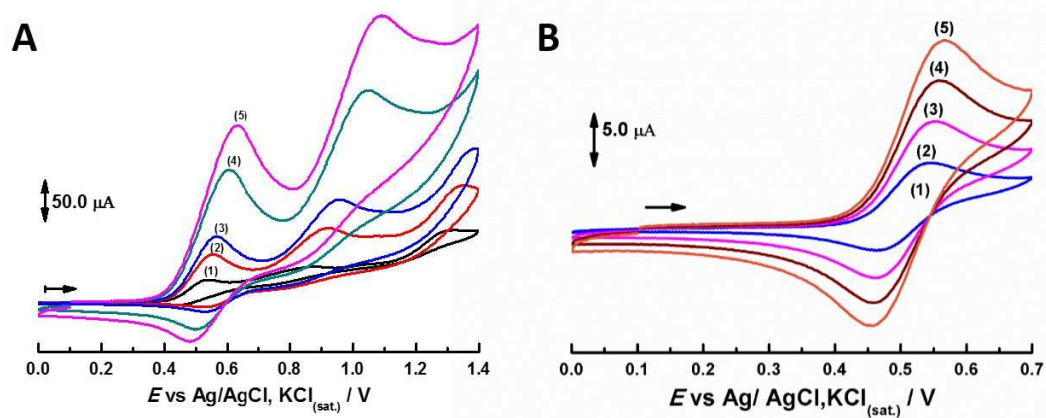






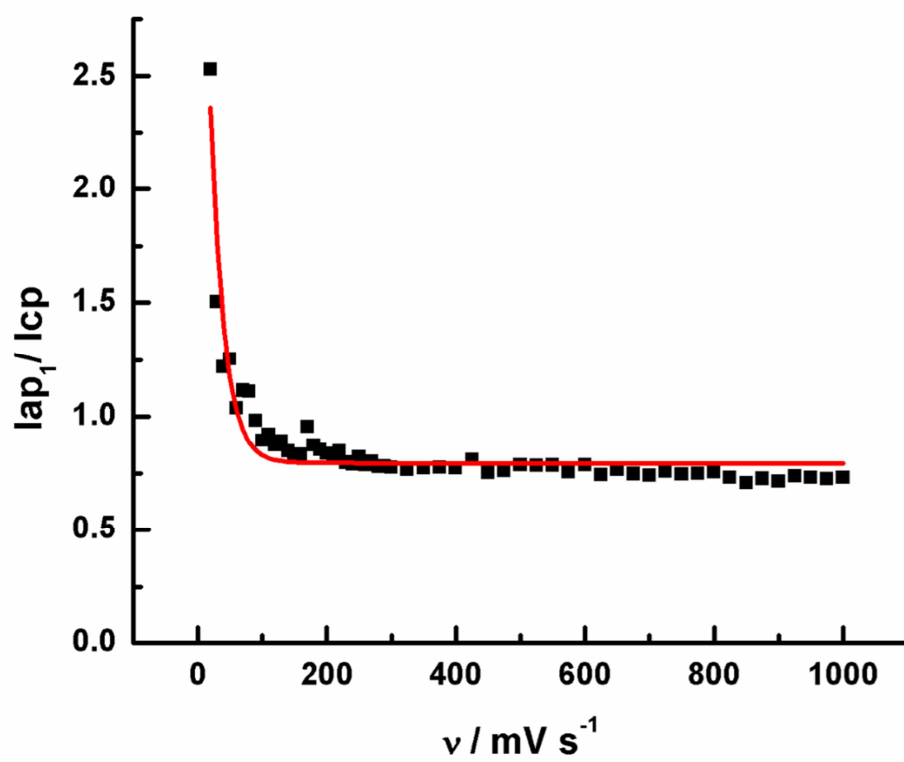


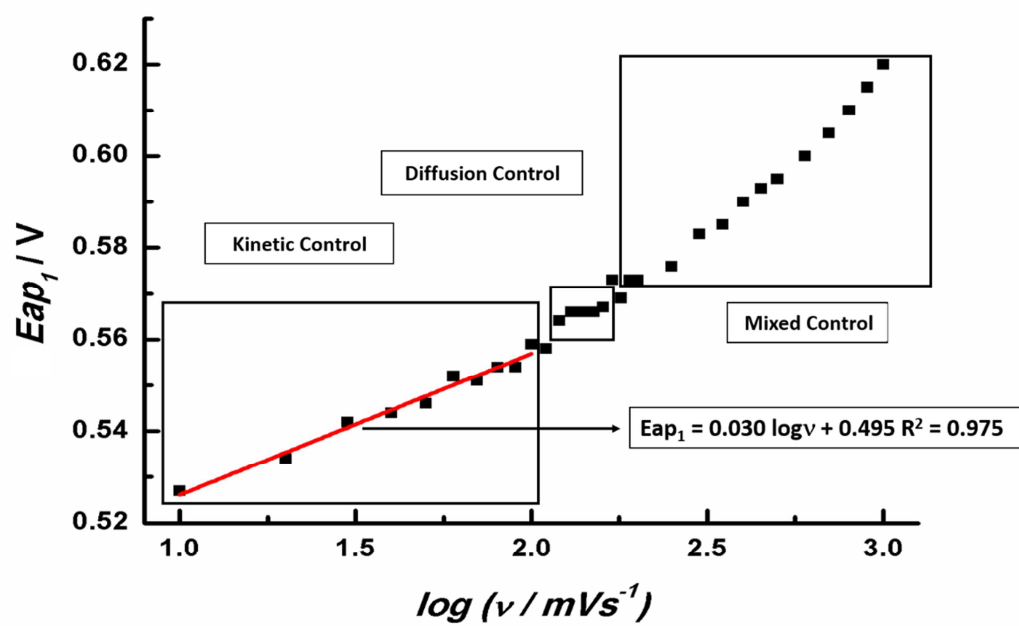


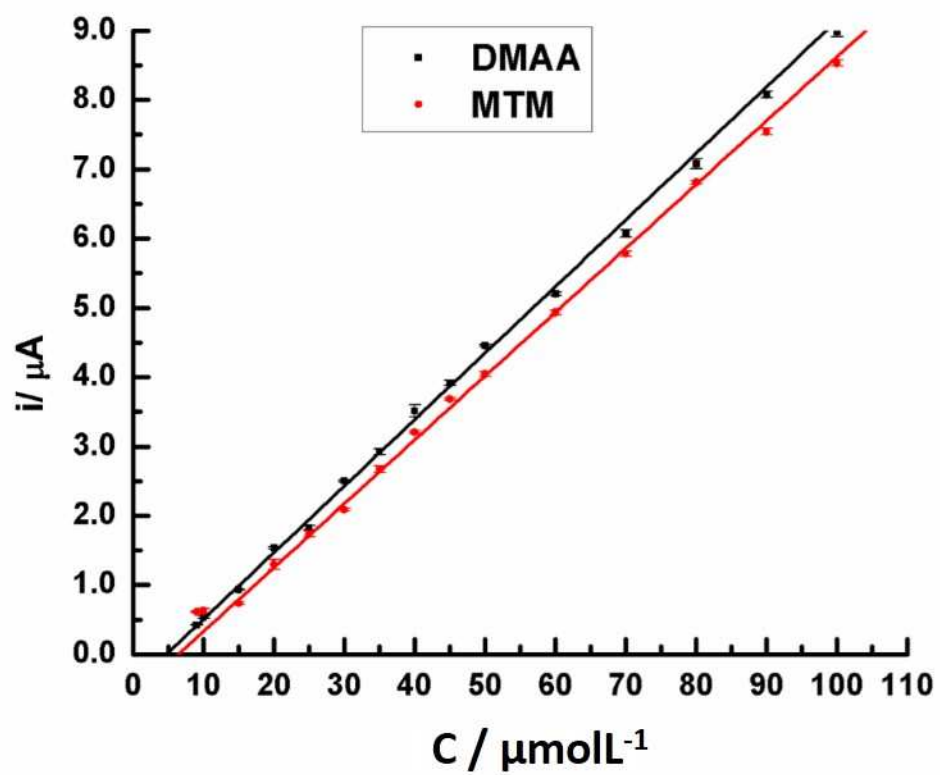


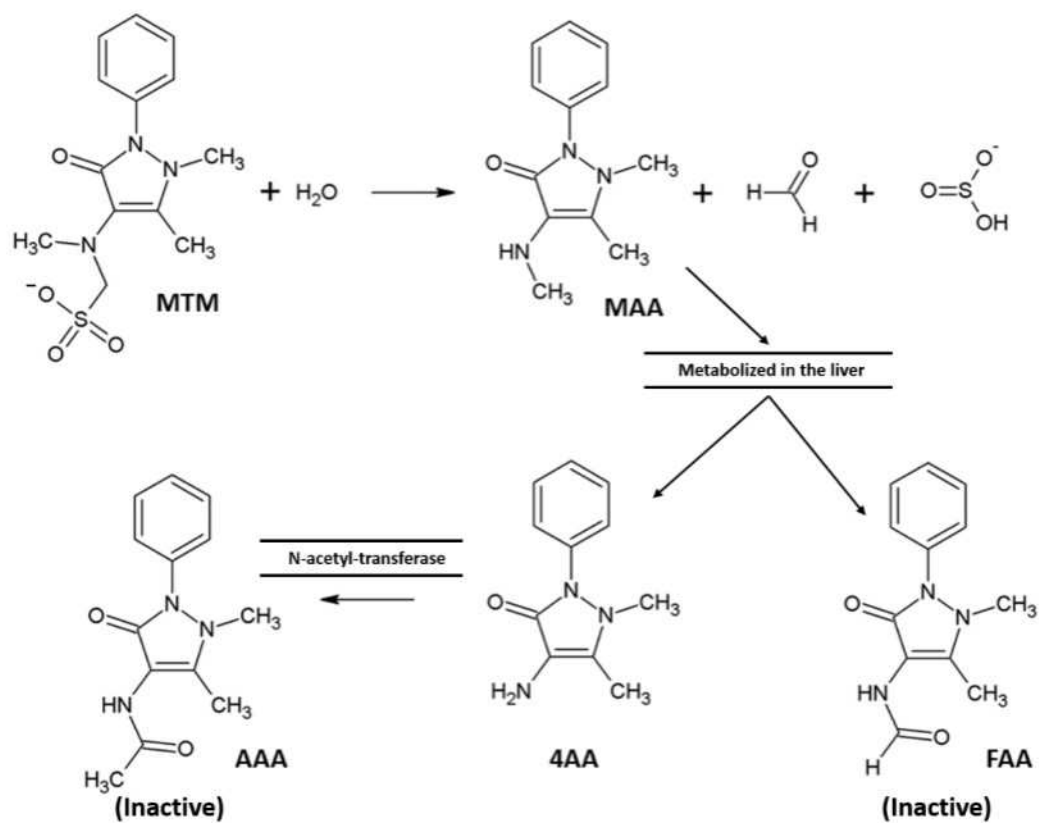
ACCEPTED MANUSCRIPT

A

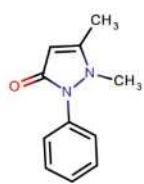
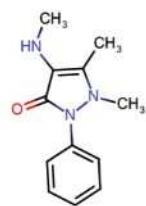
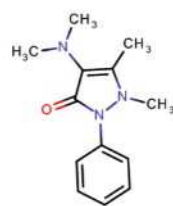
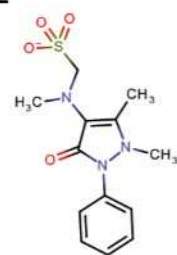




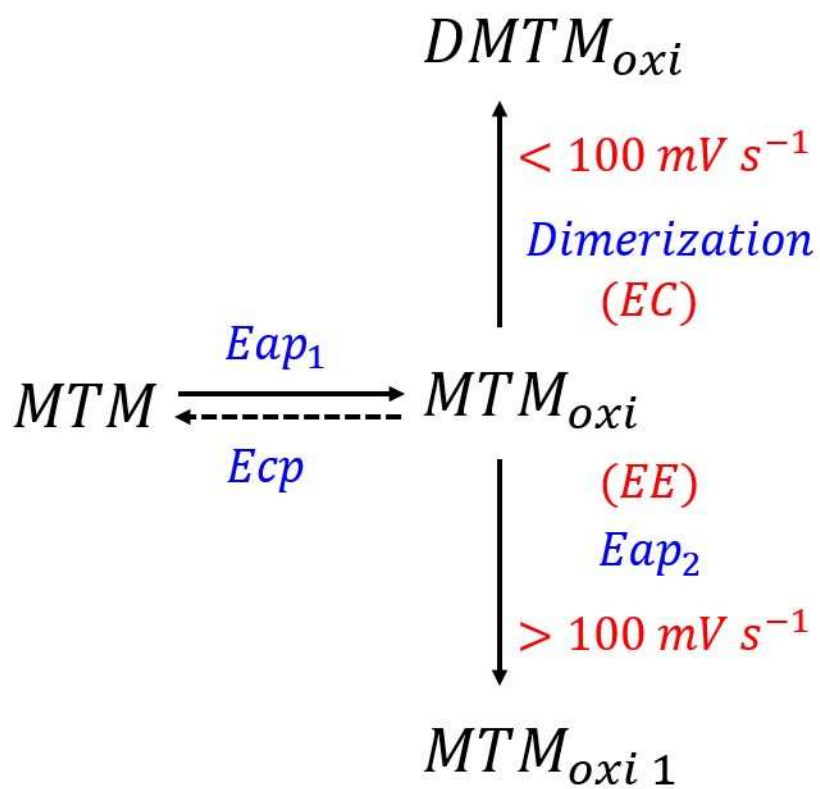


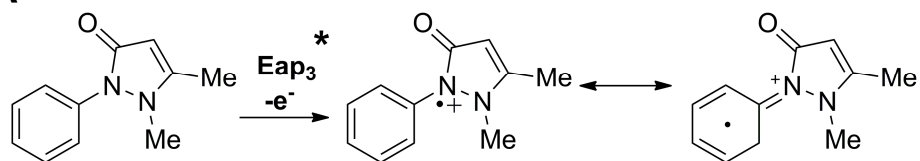
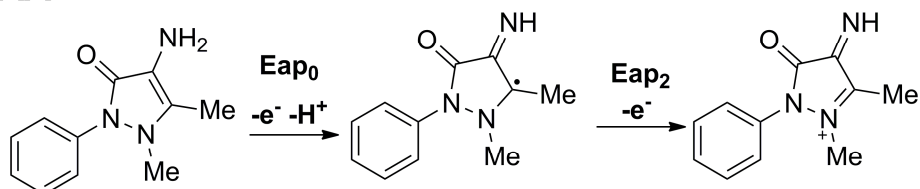
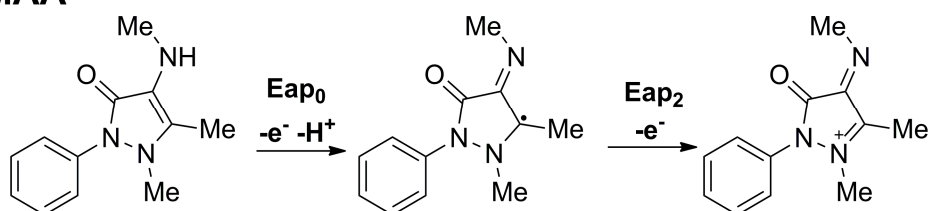
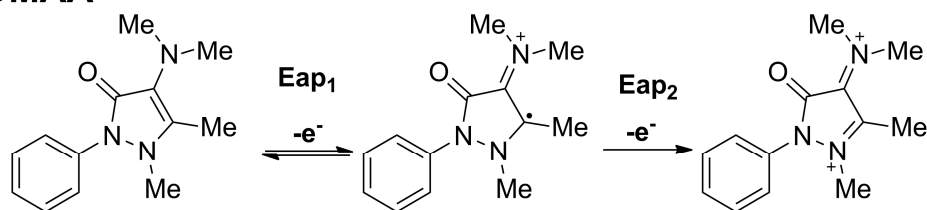
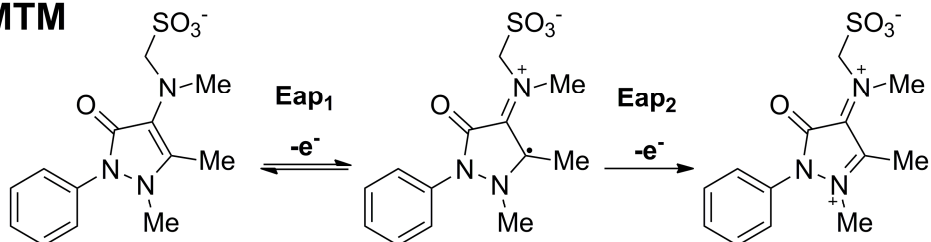


ACCEPTED M

A**AA****B****4AA****C****MAA****D****DMAA****E****MTM**

ACCEPTED MANUSCRIPT



AA**4AA****MAA****DMAA****MTM*** All the pyrazolones present Eap_3

Research Highlights

1. The MTM and the pyrazolones shows up to four oxidation electrochemical processes.
2. An electrochemical mechanism to the antipyrine group oxidation was proposed.
3. DMAA in aqueous medium can simulate the MTM in aprotic medium to quantify MTM.
4. The strength of the reducing agents follows the order $MAA > 4AA > DMAA > MTM > AA$.